# Defense Technical Information Center Compilation Part Notice

# ADP012497

TITLE: Design and Test of a Beam Line for Extraction of Slow Antiprotons from a Multi-Ring Electrode Ion Trap

DISTRIBUTION: Approved for public release, distribution unlimited

This paper is part of the following report:

TITLE: Non-Neutral Plasma Physics 4. Workshop on Non-Neutral Plasmas [2001] Held in San Diego, California on 30 July-2 August 2001

To order the complete compilation report, use: ADA404831

The component part is provided here to allow users access to individually authored sections of proceedings, annals, symposia, etc. However, the component should be considered within the context of the overall compilation report and not as a stand-alone technical report.

The following component part numbers comprise the compilation report:
ADP012489 thru ADP012577

# Design And Test Of A Beam Line For Extraction Of Slow Antiprotons From A Multi-Ring Electrode Ion Trap

K. Yoshiki Franzen[1,2], H. Higaki[2], T. Ichioka[2], M. Hori[3], Z. Wang[2], N. Kuroda[2], S. Yoneda[2], H. A. Torii[2], K. Komaki[2] and Y. Yamazaki[1,2]

[1]*Atomic Physics Laboratory, RIKEN, Wako 351-01, Japan*
[2]*Institute of Physics, University of Tokyo, Komaba 3-8-1, Meguro-ku, Tokyo, Japan*
[3]*CERN, CH-1211 Geneva 23, Switzerland*

**Abstract.** A new monoenergetic slow antiproton beam facility has recently been installed at the CERN Antiproton Decelerator (AD). The system is designed to deliver pulsed or continuous antiproton beams in the 10-1000 eV energy region which is suitable for various interesting atomic and molecular spectroscopic and collision studies. The antiprotons obtained from the AD are slowed down to around 100 keV by passing the Radio Frequency Quadrupole Decelerator (RFQD) and then captured in a multi-ring electrode ion trap. After electron cooling down to a few eV, the antiprotons will be extracted out from the trap into a collision chamber via a differential pumping system. In this paper, we present recent results in which the antiproton capture and cooling phases of this scheme have been successfully demonstrated. Furthermore, the design and tests of the extraction and differential pumping system are presented.

## INTRODUCTION

A new monoenergetic slow antiproton beam facility has recently been installed at the CERN Antiproton Decelerator (AD) [1]. The system is designed to deliver pulsed or continuous antiproton beams in the 10-1000 eV energy region which is suitable for several interesting atomic and molecular spectroscopic and collision studies. Such a slow antiproton beam will be produced in several steps [2,3]. The antiprotons are initially provided by the CERN Antiproton Decelerator (AD) ring at 5.3 MeV/u and slowed down to around 100 keV when passing through a Radio Frequency Quadrupole Decelerator (RFQD). The beam is further slowed down to around 10 keV by passing a degrader foil. The particles are then trapped inside a multi-ring electrode trap. In the trap the confined antiprotons form a non-neutral two-component plasma together with previously trapped and synchrotron radiation cooled electrons. This configuration eventually causes electron cooling of the antiprotons down to a kinetic energy of the order of 1 eV. The cooled antiprotons are then to be extracted and transported to an experimental chamber where the beam intersects with an atomic or molecular gas target beam. However, since it is unavoidable to have a relatively high background pressure in the collision chamber ($\sim 10^{-6}$ Torr) and the required pressure inside the trap must be very low ($<10^{-11}$ Torr), it is necessary to

CP606, *Non-Neutral Plasma Physics IV,* edited by F. Anderegg et al.

utilize a transport beam line equipped with a differential pumping system between the two regions. One of the difficulties with extraction of charged particles starting inside a solenoidal magnetic field is that the unguided trajectories tend to follow the field lines, which are strongly diverging at the ends of the magnet. Furthermore, focusing of the beam even outside the magnetic field is in general limited which is a direct consequence of the conservation of total angular momentum. In addition, the finite dimension of the plasma source must be considered in any realistic extraction scheme.

## EXPERIMENT

The ion trap consists of a set of ring electrodes positioned coaxially inside the bore tube of an Oxford 5 T superconducting solenoid magnet. See Fig. 1. The details of the design of the electrodes and the cabling system have been previously reported [2-5]. The size of the magnet coil is approximately 1.8 m in length and 22 cm in inner diameter. The pressure measured outside the bore tube has typically been around $2 \times 10^{-10}$ Torr. However, since the temperature of the bore tube can be lowered to around 10 K or even lower during measurements it is expected that the pressure in the trap region is at least one order lower than this value. A 200 $\mu g/cm^2$ carbon degrader foil is positioned 60 cm upstream of the magnet center which is used to degrade the antiproton beam received from the AD via the RFQ decelerator. Electrons are injected by a Spindt-type electron emitter [6] from down stream of the magnet coil, a few cm off the magnet axis and guided by the converging magnetic field into the trap region. A set of Cherenkov counters and plastic scintillator track detectors were positioned outside the magnet in order to monitor the time of arrivals and positions of charged pions emitted after antiproton annihilations [7].

The design of the extraction beam line was based on detailed Monte-Carlo simulations using a commercial software by Field Precision, which works well within a PC environment. By defining the geometries of the solenoid coil and the electrostatic

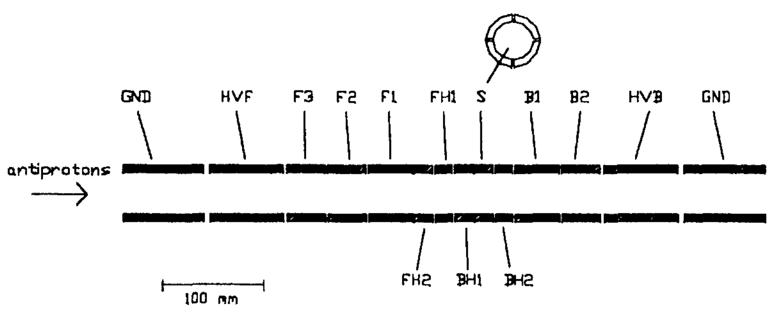


**FIGURE 1**. Schematic cross section of the ASACUSA trap electrodes. The electrode named S is segmented into four pieces.

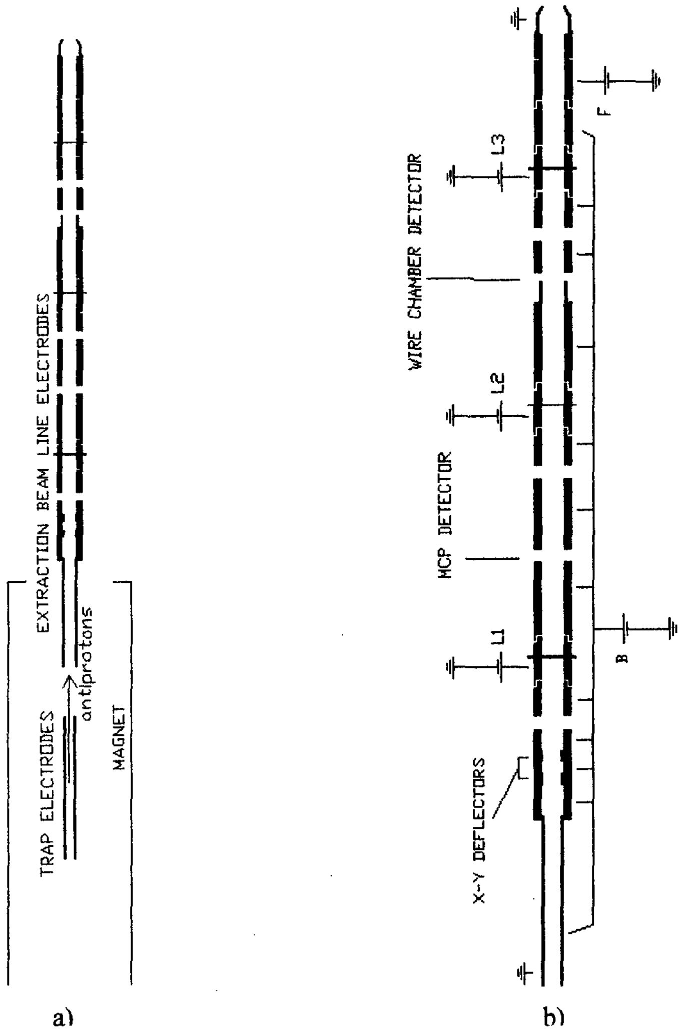


**FIGURE 2.** Schematic cross sections of a) the ASACUSA trap and extraction beam line electrodes and b) the extraction beam line electrodes. The beam travels from down to up in the figure. See the text for further information.

lenses and also by defining the current density and respective voltages, dense matrices representing both the static magnetic and electric fields were obtained. The initial conditions of a large number of antiprotons representing the plasma source were defined by assuming an antiproton plasma in the trap of a cylindrical shape with 2 mm in diameter and of homogenous density. Furthermore, it was assumed that the antiprotons have energies of 1 eV in the perpendicular direction relative to the magnetic field. The trajectories of the antiprotons extracted from the trap region were then calculated and the focal properties of the beam in the target chamber were estimated at several extraction energies. An optimized configuration could be found for maximum transport and focusing at the beam intersection point in the experimental chamber. See Table 1. The effective values of the diameters are given by $4x_{rms}$ where $x_{rms}$ is given by the root-mean-square of one transversal coordinate at the focal point for all the studied trajectories. The effective values of the divergence angles are given by $2x'_{rms}$ where $x'_{rms}$ is given by the root-mean-square of the slopes relative to the beam line axis at the focal point for the same trajectories [8]. Minimization of these values, each representing an envelope of the respective beam parameter, while keeping a 100% transmission efficiency of the system were the main criteria of the design. In addition all the practical requirements on vacuum, high voltage electrostatic lenses, materials etc. were taken into account. A schematic overview of the resulting design can be observed in Fig. 2.

After capture and cooling, the antiprotons are extracted from the trap by raising the potentials of electrodes F2, F1, FH2, FH1, BH1, S, BH2 and B1 up to the potential of electrode B2, which is kept lower than the potential of electrode F3 (see Fig. 1). The electrodes HVF and HVB are at this stage kept at ground potential. The antiprotons then enter the beam line electrode system, which penetrates into the homogenous part of the solenoidal magnetic field as illustrated in Fig. 2a. After passing a grounded electrode the antiprotons reach the electrodes with a potential B, which accelerates or decelerates the antiprotons to a kinetic energy of few hundreds eV inside the beam line, see Fig. 2b. Around this position they also pass a double set of electrostatic x-y deflectors, which provides a mean to align the trajectories against the beam line axis. The beam then reaches electrodes and an aperture, which are kept at a potential L1 as can be seen in Fig. 2b. Here a cylindrically symmetric accelerating electric field forces the beam to pass the aperture, which is high voltage floatable and of adjustable size. The typical maximum kinetic energy of the beam around the aperture is a few keV. Exiting the aperture the beam is decelerated down to a few hundreds eV. This deceleration provides further focusing which at correctly applied potentials makes the antiprotons leave the lens system again as a parallel beam. With an aperture size of 4 mm in diameter it is estimated that the pressure downstream of the aperture can be kept around 100 times as high as the pressure upstream. The

**TABLE 1. Antiproton beam focus parameters versus extraction energy.**

| Extraction energy (eV) | Effective beam diameter (mm) | Effective divergence angle (deg) |
|---|---|---|
| 10 | 6 | ±18 |
| 100 | 5 | ±6.5 |
| 250 | 4 | ±4.9 |

minimum measured background pressure after baking in the downstream region is in the $10^{-10}$ Torr region, which is obtained by a 1000 l/s turbo molecular pump. The functions of the lens systems kept at the potentials L2 and L3 in Fig. 2b are exactly the same as for the one just described. Down stream of the aperture kept at the potential L2 a 400 l/s turbo molecular pump gives a background pressure in the $10^{-9}$ Torr range while turbo molecular pumps installed in an experimental chamber will provide the pumping downstream of the aperture at potential L3. The three apertures set at sizes around 4 mm in diameter thus provide the required differential pumping efficiency. The beam is finally focused into the experimental chamber by passing the electrode at potential F and finally a grounded electrode as illustrated in Fig. 2b. The focal point of the beam is 25 mm downstream from the end of the last electrode, which is at ground potential. To eliminate any electric stray fields at this point it is possible to attach a mesh to the downstream surface of this electrode. To optimize the extraction and transportation of the beam there are two detectors installed along the beam line which functions are to monitor the beam profile. The first one, which is marked MCP DETECTOR in Fig. 2b, is a microchannel plate system equipped with a delay line anode. This will give information on both the arrival timing and the position of each detected antiproton. The downstream detector of the beam line, marked WIRE CHAMBER DETECTOR in Fig. 2b, gives the possibility to measure the beam profile during pulsed extraction while providing a high transmission.

## RESULTS

Before starting experiments with antiprotons it was shown that we could trap and compress electrons, $H^-$ and positive ion plasmas using the described trap system. During these experiments we also performed non-neutral plasma diagnosis by utilizing a tank circuit. These results are described in detail elsewhere [4]. During our first four weeks of AD beam time in June 2001 the following results were acquired.

Fig 3a exhibits the signal from a Cherenkov counter detector positioned close to the end of the magnet closest to the RFQD. At this end a gate valve is mounted which in this case was closed, thus blocking the beam. The time scale is relative to a given start signal which is correlated to the arrival of antiprotons kicked out from the AD. As can be observed, pulses arrived and annihilated against the gate valve at 1.25 μs and at 1.75 μs, each corresponding to incoming antiprotons of 5 MeV and 85 keV energies respectively. The pulse with the lower energy corresponds to antiprotons decelerated by the RFQ Decelerator. By observing the corresponding signal from a Cherenkov counter positioned close to the gate valve mounted at the opposite end of the magnet and with the other gate valve opened an additional broader feature was found at around 3-5 μs, see Fig. 3b. This indicates that the antiprotons had undergone further deceleration due to passage through the carbon degrader foil when entering the magnet. The energy corresponding to the position of this peak is 20 keV and lower. By applying a –10 kV potential to the trap electrode HVB as seen in Fig.1, it was observed that the low energy tail of the degraded energy peak was reduced. This is

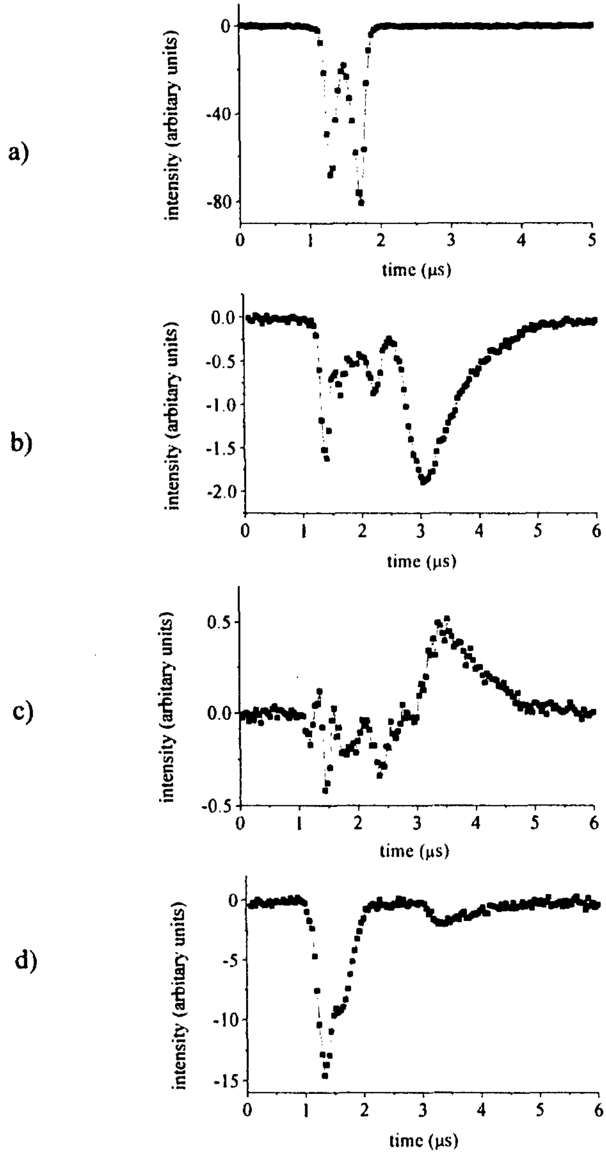


**FIGURE 3.** Signals acquired with a Cherenkov counter a) positioned upstream of the trap with the upstream gate valve closed, b) positioned downstream of the trap with the upstream gate valve opened, c) positioned downstream of the trap showing the difference between with and without –10 kV applied to electrode HVB and d) positioned upstream of the trap with the upstream gate valve opened and with –10 kV applied to electrode HVB. See the text for further information.

illustrated in Fig. 3c, which is a spectrum showing the signal difference obtained with the high voltage on and off. The peak with a maximum at 3.5 μs is thus explained by reflection of low energy antiprotons towards the entrance end of the magnet. This was confirmed by again observing the signal from the upstream Cherenkov counter, which showed an additional low energy peak when high voltage was applied (see Fig. 3d).

The next step was to confirm confinement of antiprotons. For this purpose the plastic scintillator detectors were positioned in parallel to the magnet axis. By applying the −10 kV potentials to the electrode HVF (see Fig. 1) of the trap before the reflected antiprotons could escape as in Fig. 3d they could be trapped. After 1 s they were released by removing the high voltage potentials, which quickly resulted in annihilation as can be seen in Fig. 4a. A rough estimate of the number of captured antiprotons is given by counting the number of pulses within the peak around 1 s and by taking the solid angle of the detector and the multiplicity of the charged pions emitted after annihilation into account. This gives a number around 300000

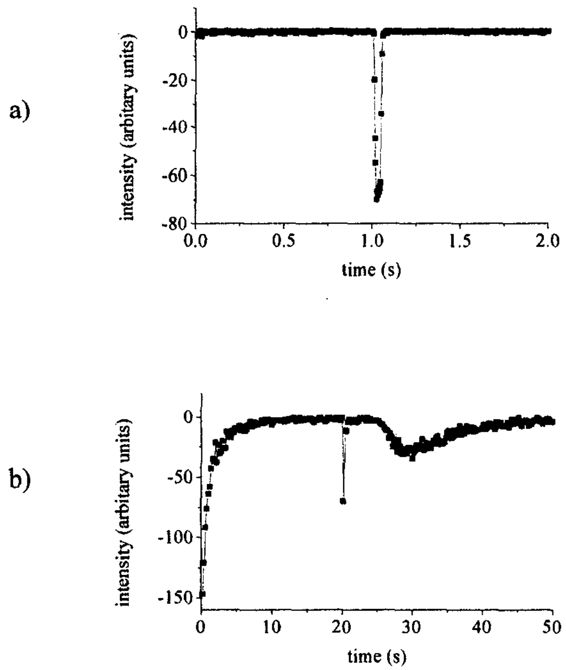


**FIGURE 4.** Signals acquired with a plastic scintillator detector positioned parallel to the trap magnet. The panels show a) antiprotons annihilating after 1 s trapping time and b) electron cooled antiprotons confined in a well of 100 V depth after the −10 kV high voltages applied to the end electrodes of the trap have been turned off after 20 s trapping time.

antiprotons captured from one shot. Furthermore, it was also shown that we could cool down the captured antiprotons to less than 100 eV and probably much less. This is exhibited in Fig. 4b, which again shows the signal acquired with the plastic scintillator detector. However, 50 s before the antiprotons were captured, 60 eV electrons were injected and confined within the trap region. Previous experiments had shown that the number of trapped electrons during identical conditions was of the order of $10^8$. At the high magnetic field utilized in these series of measurements (3.3 T) the electrons quickly loses their kinetic energy due to synchrotron radiation. The –10 kV high voltage potentials applied to the end electrodes of the trap was turned off at 20 s after the antiproton injection which can be seen in Fig. 4b as a narrow peak. However, a well of depth 100 V was kept on until 50 s after the injection. It can be clearly seen in the figure how the annihilation continues up to this time, which shows that there are still antiprotons inside the trap region after the high voltage has been turned off.

Our next goal during the allocated AD beam time in October 2001 will include extraction studies of the slow antiprotons. Here we briefly report on experiments in which the above-described system was used to extract slow positive ions from the trap to the focal point. By ionizing the residual gas inside the trap region with the electron beam, positive ions were created and trapped. These ions were extracted from the trap by using the same procedure as previously described for antiproton extraction but with the opposite sign of the applied potentials. For instance, the potential applied to the

a)

b)

c)

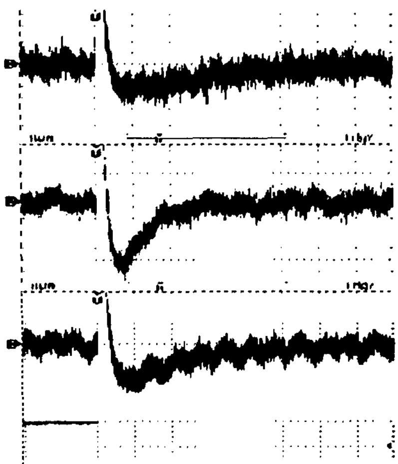

**FIGURE 5.** The raw signal obtained from the second aperture via a charge amplifier with potential L1 set to a) –500 V, b) –3410 V, and c) –4500 V. The changing trap well potential was used as a trigger pulse. The vertical scale is 500 mV/div and the horizontal scale is 10 ms/div. The gain of the charge amplifier is 164 mV per $10^6$ charged particles.

trap electrode B2 was in one case set to 500 V. The ions then entered the extraction beam line electrodes with kinetic energies around 500 eV and were decelerated down to around 250 eV by setting B in Fig. 2b to a potential 250 V. The positive ions reaching the aperture of the lens L2 (Fig. 2b), which in this case served as a Faraday cup, were monitored with a charge amplifier while varying the potential L1. As can be observed in Fig. 5 there is certainly a dependence on the applied potential L1 and the maximum throughput was obtained at L1=-3410 V, which is the value predicted by the calculations. By utilizing the second and third lens systems (marked by L2 and L3 in Fig. 2b) the extracted ions were transported to the focal point of the beam line where the current of positive ions reaching the surface of a MCP detector was measured. A rough estimate gives that $10^5$ positive ions per extraction reached the focal point at 250, 100 and 10 eV extraction energies with the apertures set at 6 mm in diameter.

In addition slow extraction tests monitoring the beam profile after the first aperture with the MCP detector system (see Fig. 2b) equipped with a delay line anode were performed. Figure 6 shows some examples of these results acquired during similar conditions except for different L1 voltages (see Fig. 2b). The ions were extracted at 250 eV. According to the discussed calculations the transmittance of the beam should at this extraction energy be at maximum for L1=-3640 V. This seems to be confirmed by the experiment since the measurements with L1=-3000 V (Fig. 6a) and L1=-4000 V (Fig. 6c) both exhibit a weaker signal compared with the case of a correctly applied potential (Fig. 6b). During these tests, the positive ions were extracted very slowly from the trap, even during periods up to several tens of seconds. It was observed that the current and the beam profile remained almost constant during the extraction. A similar detector is presently being prepared in order to monitor the antiproton beam profile measured at the focal point of the beam line.

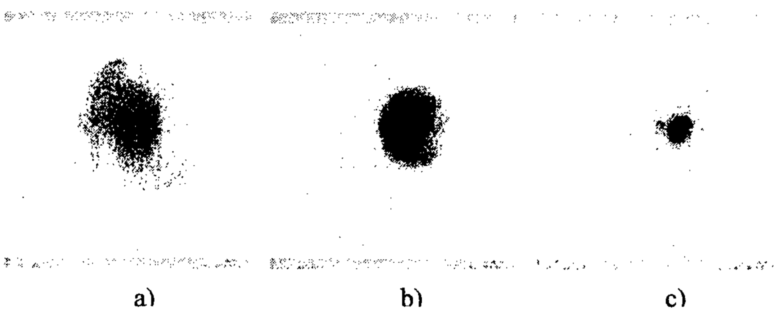


**FIGURE 6.** The beam profile as measured by a position sensitive MCP detector during slow extraction of positive ions from the trap via an aperture of 4 mm in diameter. The applied potentials L1 were a) –3000 V, b) –3640 V (optimized according to calculations) and c) –4000 V.

## CONCLUSIONS

The most important technical features of the slow antiproton extraction beam line were described. Recent results of the antiproton capture and cooling phases were presented. Furthermore, preliminary test results of the extraction beam line using positive ions were presented showing the possibility to extract charged particles as a slow beam from the trap via a three-stage differential pumping system. The system is now ready to be tested and optimized for the delivery of a slow antiproton beam at CERN.


## ACKNOWLEDGMENTS

We are most grateful to the Antiproton Decelerator (AD) staff at CERN for providing us with the antiproton beam.

Postdoctoral Fellowships from the Japanese Society for the Promotion of Science (JSPS) and the Science and Technology Agency (STA) financially supported four of the authors (K.Y.F., H.H., M.H. and Z.W.) during these experiments.


## REFERENCES


1. Baird S. et al., "Design study of the antiproton decelerator", in *Ad. Technical Report*, edited by Maury S., CERN/PS 96-43 (AR), CERN, 1996
2. Yamazaki Y., *NIM B* **154** 174-184 (1999)
3. Yamazaki Y., "Antiprotons and the ASACUSA project", in *Non-Neutral Plasma Physics III*, edited by Bollinger J. J. et al., AIP Conference Proceedings 498, New York, 1999, pp. 48-58
4. Ichioka T., Higaki H., Hori M., Oshima N., Kuroki K, Mohri A., Komaki K. and Yamazaki Y., "Multi-ring trap as a reservoir of cooled antiprotons", in *Non-Neutral Plasma Physics III*, edited by Bollinger J. J. et al., AIP Conference Proceedings 498, New York, 1999, pp. 59-64
5. Ichioka T., Ph.D. thesis, University of Tokyo, 2001
6. Spindt C. A. et al., *IEEE Trans. On Elec. Dev.* **38** 2355-2363 (1991)
7. Leo W. R., *Techniques for Nuclear and Particle Physics Experiments*, Springer-Verlag, Berlin, 1994, pp. 36-37 and pp. 157-213
8. Reiser M., *Theory and Design of Charged Particle Beams*, John Wiley & Sons, New York, 1994, pp. 59